Electron Diffraction Self-Imaging of Molecular Fragmentation in Two-Step Double Ionization of Water

H. Sann,[1] T. Jahnke,[1] T. Havermeier,[1] K. Kreidi,[1] C. Stuck,[1] M. Meckel,[1] M. S. Schöffler,[1] N. Neumann,[1]
R. Wallauer,[1] S. Voss,[1] A. Czasch,[1] O. Jagutzki,[1] Th. Weber,[1] H. Schmidt-Böcking,[1] S. Miyabe,[2]
D. J. Haxton,[2] A. E. Orel,[3] T. N. Rescigno,[2] and R. Dörner[1],*

[1]*Institut für Kernphysik, J. W. Goethe Universität, Max-von-Laue-Str. 1, 60438 Frankfurt, Germany*
[2]*Lawrence Berkeley National Laboratory, Chemical Sciences and Ultrafast X-ray Science Laboratory,
Berkeley, California 94720, USA*
[3]*Department of Applied Science, University of California, Davis, California 95616, USA*
(Received 10 December 2010; published 29 March 2011)

We doubly ionize H_2O by single photon absorption at 43 eV leading to $H^+ + OH^+$. A direct double ionization and a sequential process in which single ionization is followed by rapid dissociation into a proton and an autoionizing OH^* are identified. The angular distribution of this delayed autoionization electron shows a preferred emission in the direction of the emitted proton. From this diffraction feature we obtain internuclear distances of 700 to 1100 a.u. at which the autoionization of the OH^* occurs. The experimental findings are in line with calculations of the excited potential energy surfaces and their lifetimes.

Excited neutral atoms, molecules or clusters can relax by emission of an autoionization electron, once the excitation energy is above the ionization potential. If the excited system however is positively charged, autoionization can be energetically blocked by the coulomb attraction. This coulomb blockade is lifted if the excited system neutralizes by emission of a cation. After the cation has taken the positive charge far enough away, the blocked autoionization channel of the now neutral system can open leading to a time delayed emission of a low energy auto-ionization electron. Experimental evidence for this very general scenario has been reported in pioneering experiments on photo double ionization of water [1] and has been confirmed for other small molecules [2,3]. For O_2 such time delayed autoionization has recently been followed in real time [4].

In the present letter we show that the time delayed auto-ionization can lead to a characteristic angular distribution of this autoionization electron. It shows a pronounced peak in the direction to which the positive charge has left the system. If the cation is far (> 200 a.u.) from the excited neutral fragment when the latter autoionizes, the slow auto-ionization electron takes a characteristic diffraction image of the expelled cation.

To this end we doubly photoionize H_2O at a photon energy of $h\nu = 43$ eV. Above the vertical double ioniza-tion threshold of approximately 39 eV [1,5] the ejection of the two electrons can either be simultaneous [Eq. (1)], moderated by electron correlation, or via the two-step process introduced above [Eq. (2)].

$$h\nu + H_2O \rightarrow H^+ + OH^+ + 2e^-, \quad (1)$$

$$h\nu + H_2O \rightarrow H^+ + OH^* + e^- \rightarrow H^+ + OH^+ + 2e^-. \quad (2)$$
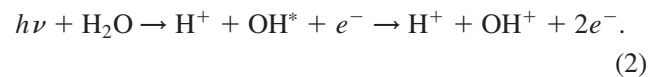
The latter process has a threshold at 34.4 eV [1,2,5].

By detecting the directions and energies of all particles in coincidence we distinguish pathways (1) and (2). We select events where the double ionization occurs in two steps and measure the energy and angular distribution of the autoionization electron with respect to the direction in which the proton is expelled.

The experiment was performed at the BESSY synchro-tron radiation source U125/2 SGM in single bunch operation using the COLTRIMS technique [6–8]. Linearly polarized photons are focussed into a supersonic H_2O gas jet, prepared by expanding water vapour through a 60 μm nozzle at a temperature of 110 °C. Electrons and ions created in the interaction region are guided by homo-genous electric ($E = 10$ V/cm) and magnetic fields ($B = 7$ Gauss) onto two Roentdek position sensitive multi-hit micro channel plate detectors [9]. The electron arm of the analyzer employed McLaren-time focussing [10] and a hexagonal delayline anode [11] was used in order to reduce the dead time of the electron detector.

In Fig. 1 we show the energy correlation between the electrons and ions. We exploit this information to identify the final states and distinguish channel (1) from (2). By energy conservation, the final energy (electronic + vibrational + rotational) of the OH^+ is given by

$$E_{OH} = h\nu - E_b - IP_H - IP_{OH} - KER - E_1 - E_2, \quad (3)$$

where $E_b = 5.1$ eV is the dissociation energy needed to split H_2O to H and OH, $IP_H = 13.6$ eV and $IP_{OH} = 13.0$ eV are the ionization potentials of ground-state
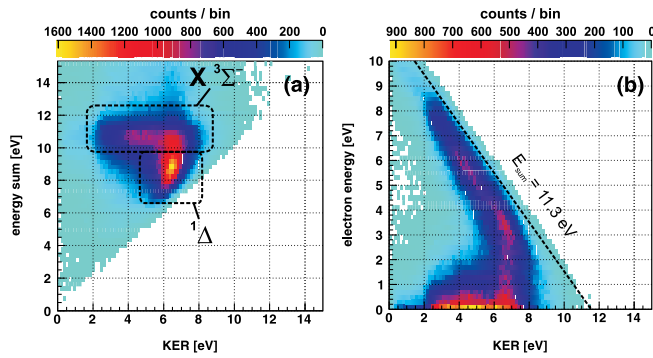
FIG. 1 (color online).   Energy correlation of both electrons and OH^+ and H^+ for photo double ionization of H_2O at $h\nu = 43$ eV. (a) Horizontal axis: kinetic energy release, vertical axis: sum energy of both electrons and both ions. (b) Horizontal axis: kinetic energy release, vertical axis: energy of one of the two electrons. In (b) only events leading to the $X^3\Sigma^-$ ground state are plotted.

H and OH, KER is the measured kinetic energy release of the ionic fragments, E_1 and E_2 are the also measured kinetic energies of the two electrons. Figure 1(a) shows that the OH^+ is created in its two lowest electronic states ($X^3\Sigma^-$ and $^1\Delta$). As one can see the KER distribution is very different for the two final states of OH^+. To unravel the corresponding double ionization mechanisms we plot the energy of one of the two electrons versus the KER. For events leading to the $X^3\Sigma^-$ ground state this is shown in Fig. 1(b). By energy conservation the region of valid events is constrained by the diagonal indicated in the figure ($h\nu - E_b - IP_H - IP_{OH} = 11.3$ eV). The peak at KER = 6.5 eV corresponds to a pair of electrons which share their energy continuously. Such continuous energy distribution is characteristic of a direct double ionization where both electrons are ejected simultaneously, mediated by electron correlation [12]. This is in striking contrast to the energy distribution in the interval KER = 1–6 eV. In this region a low energy electron is created which is almost independent of the KER associated with a fast electron whose energy is roughly 10.5 eV—KER. Upon variation of the photon energy the low energy electron remains unchanged while the fast electron changes in energy (not shown). From this we can unambiguously conclude that the fast electron is a direct photoelectron. The photoabsorption launches the electron into the continuum and leaves the molecule on a steeply repulsive region of an H_2O^{+*} potential energy surface. The vertical ionization potential which determines the electron energy then depends on the HO-H bond length at the instant of photo absorption. The energy of the slow electron in contrast does not depend on the KER. For events leading to the $^1\Delta$ state we observe only one peak at KER = 6.5 eV with all electron pairs sharing their energy continuously (not shown). This implies that the two-step process always leads to the electronic ground state of OH^+ while the direct process also populates the first excited state. In the
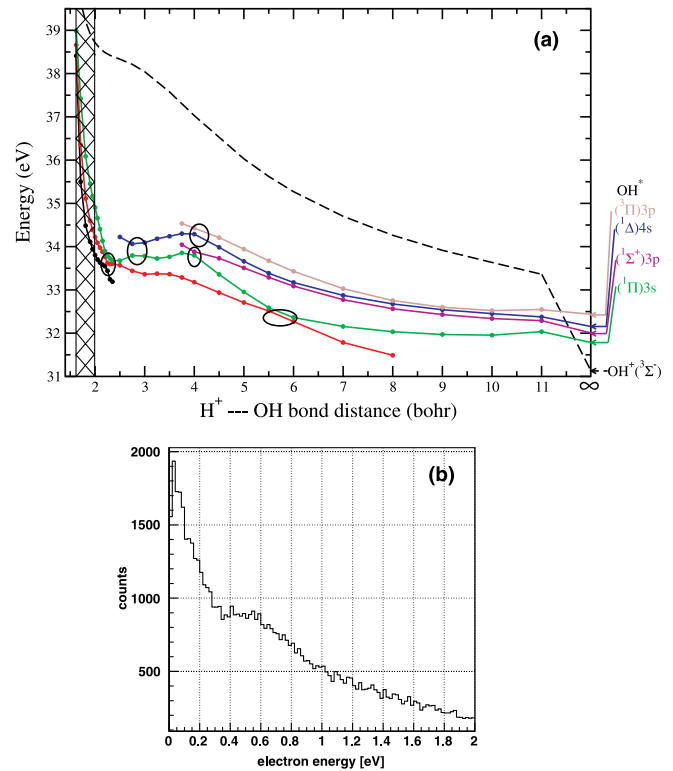

FIG. 2 (color online).   (a) Potential energy surface of the relevant states of H^+-OH^*. One OH bond distance and the H-O-H angle are frozen at the H_2O equilibrium value. The Franck-Condon region is indicated by cross-hatched area and circles denote areas of avoided crossings. Dashed curve is ground-state H_2O^{++}. (b) Electron energy distribution for the region KER = 2–5 eV.

remainder of this letter we will concentrate on events leading to the ground state.

To identify the states involved in the autoionization we carried out multireference configuration-interaction calculations for potential energy curves of H_2O^+ in this region [Fig. 2(a)]. We held the H-O-H angle and one OH bond distance frozen at their H_2O equilibrium values. We find three excited H_2O^+ states of $2A'$ symmetry which all have substantial oxygen $2s$ hole character. In the Franck-Condon region they are 35–39 eV above the H_2O ground state, which leads to the observed photoelectron energies of 4–8 eV [Fig. 1(b)] at the present photon energy. These three states, which undergo several avoided crossings as the H-OH distance increases (marked by circles in Fig. 2(a)], can feed four states which dissociate to $H^+ + OH^*$. The OH^* states—which we identify as $(^1\Pi)3s$, $(^1\Sigma^+)3p$, $(^1\Delta)4s$ and $(^3\Pi)3p$—are autoionizing states of OH with a Rydberg electron attached to a bound, excited state of OH^+. Asymptotically they lie above the $^3\Sigma^-$ OH^+ ground state, so they can decay by autoionization. Since the autoionizing OH^* states can be characterized as electron—OH^+ scattering resonances, we carried out variational fixed-nuclei scattering calculations using the Complex

Kohn method to obtain the energies and widths of the autoionizing states [13]. The energies of the four autoionizing states involved were consistent with the asymptotes shown in Fig. 2(a), while the lifetimes, i.e., the inverse of the widths, ranged from 50 fs for the $(^1\Pi)3s$ state to several ps for the other states. In the experiment all of these states will be vibrationally and rotationally excited (first vibrational excitation in OH^+ is at 0.37 eV [14]), leading to a broad band of initial and final states for an Auger decay. Our experimental energy resolution is not sufficient to resolve these final vibrational excitations.

The measured energy distribution of the autoionization electron is shown in Fig. 2(b). This spectrum only contains events for which the KER is between 2 and 5 eV. It shows a steep decrease from zero and an additional feature at about 0.5 eV. According to the Franck-Condon principle ionization of the water molecule can take place at internuclear distances of up to 2 a.u. In ionization processes leading to the lowest state shown in Fig. 2(a) this corresponds to a resulting KER of 2 eV. This is in agreement with the measured minimum KER [Fig. 1(b)].

We get additional information on the decay from the angular distribution of the low energy autoionization electrons with respect to the momentum vector of the proton (Fig. 3). It shows an almost isotropic background with a distinct "nose" in the direction of the proton. We find that this feature prevails for the whole region of KER = 2–5 eV and electron energy from 0.05 to 2 eV. The angular distribution of the photoelectrons does not have this noselike feature (not shown).
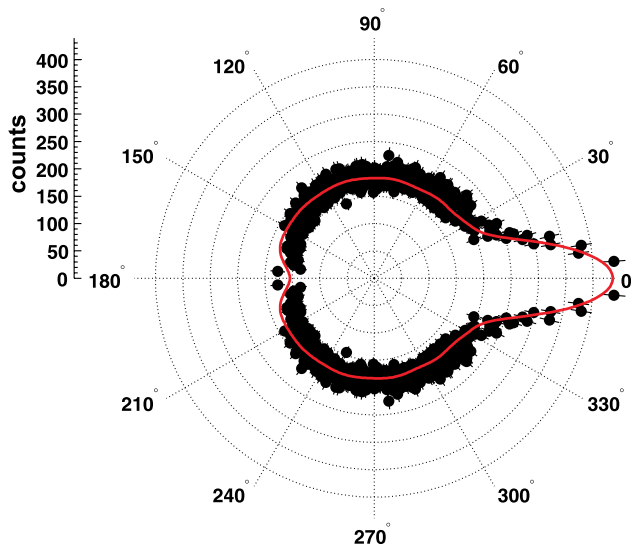

FIG. 3 (color online). Measured distribution of the angle between the electron and the proton direction for electron energies between 0.2 and 0.6 eV and KER between 2 and 5 eV. Black dots experiment, red line classical simulation for electron energy of 0.2–0.6 eV and internuclear distance $R = 800$ a.u. at the instant of autoionization. The simulation is convoluted with the experimental angular resolution.

Structures in the angular distribution of molecular Auger electrons are known to originate from several different effects: (i) the angular part of the wave function of the decaying state and the hole are imprinted on the Auger continuum angular distribution [15], (ii) emission from indistinguishable centers in the molecule causes interference [16] and (iii) the emerging electron can be multiply scattered in the molecular potential [17], as it is also well known for photoelectron angular distributions [18]. We now demonstrate that this last effect of electron diffraction at the distant proton leads to the formation of the noselike structure. Even for a KER as small as 2 eV, the H^+-OH separation is large compared to the extension of the OH^* state which emits the electron. Hence at the distances where the Auger electron wave experiences the proton, the potential of the OH^+ left behind is to a good approximation spherically symmetric and the internal structure of the OH^+ is less relevant for the scattering. We therefore compare the data to a simple classical scattering scenario. We launch electron trajectories radially from a sphere of 1 a.u. centered at the origin. We locate one Coulomb potential at the origin and a second one simulating the proton at a distance R. The starting kinetic energy of the electron is chosen such that the asymptotic energy matches the observed continuum energy. This classical modelling, yielding the red line in Fig. 3, reproduces the observed angular distribution almost exactly. In the simulation we have used R as a fitting parameter. The experimental angular resolution is included in the simulation.

Sample trajectories for $R = 800$ a.u. are shown in Fig. 4(a). Note that the proton does not act as a lens focusing the electrons forward [19] but rather bends the trajectories with no preference given to the forward direction. The deflection function, i.e., the asymptotic angle Θ_f at which the electron finally escapes as a function of the angle Θ_i at which it was originally launched from the origin, is shown in Fig. 4(b). For the large distance chosen here the deflection function obtained for this two center scenario is very close to the pure Rutherford scattering case in which the additional Coulomb potential at the origin is neglected. Isotropic emission of the electron in three dimensions means constant flux into all solid angle elements $d\Omega = 4\pi \sin(\theta)d\theta d\phi = 4\pi d\cos\theta d\phi$. If this solid angle effect is taken into account, the bending of an electron trajectory initially emitted on the cone at a particular value θ_i into the final forward direction ($\theta_f = 0$) leads to the increase of flux in the forward direction and the formation of the nose. The fraction of flux in the forward direction, i.e., the size of the nose, decreases with internuclear distance and electron energy [Fig. 4(c)]. We use the calculated dependence of the size of the nose on energy and R to estimate the distance R_{decay}. The experimental values for the size of the nose, i.e., the fraction of the total electron flux into 4π which is in the peak as a function of electron energy is shown by the symbols in Fig. 4(c). As expected
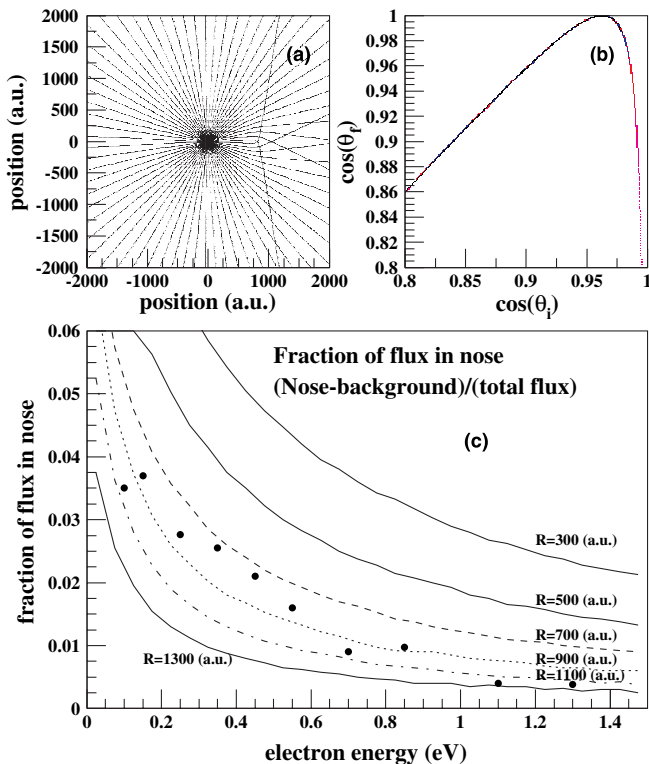
FIG. 4 (color online). (a) Sample trajectories for an electron of 0.4 eV. Two coulomb charges are located at the origin and at $x = 800$ a.u. and $y = 0$ a.u.. The electron trajectories are launched at a radius of 1 a.u. around the origin (see text). (b) Deflection function, i.e., cosine initial emission angle versus cosine of asymptotic final angle for electron energy of 0.4 eV and $R = 800$ a.u.. (c) Ratio of the flux in the noselike structure (after subtraction of the isotropic background) and the total flux in 4π as a function of electron energy. Lines: simulation for different R. Circles: experimental data.

for Rutherford scattering and also seen in the simulations, the number of experimentally observed diffracted electrons decreases with increasing electron energy. Comparing the simulations with the data, we obtain a value of $R_{decay} = 700–1100$ a.u.. Since the KER is measured, we can convert this to a time. A KER of 3 eV and a internuclear distance of 800 a.u. correspond to a delay time of approximately 2 ps between the photo absorption and the autoionization.

In conclusion, we take advantage of an anisotropy in the electron angular distribution to probe the distance between a proton and an autoionizing fragment in a dissociating molecular ion at the time when autoionization takes place. We emphasize that our experiment observes the proton in the diffraction pattern, something commonly taken to be a weak signal because scattering scales with the charge squared. We believe that the observed forward electron flux in the direction of the broken bond is rather general. It should occur whenever a positively charged fragment is emitted from a molecule or cluster and at a later time electrons are emitted. In this case the delayed electron will trace the direction of the positive fragment. This should hold, for example, for multiple ionization of clusters. This effect will also be important in all time resolved photoionization and fragmentation experiments as they will become possible with the new FEL or higher harmonic sources. Here a first pulse can initiate ionization and dissociation and the second, time delayed pulse will emit a second photoelectron. Based on our observations we predict that the forward electron flux observed in the present experiment will be ubiquitous in such time resolved electron diffraction experiments.

*doerner@atom.uni-frankfurt.de

[1] D. Winkoun, G. Dujardin, L. Hellner, and M. J. Besnard, J. Phys. B **21**, 1385 (1988).
[2] T. A. Carlson et al., J. Chem. Phys. **84**, 4755 (1986).
[3] R. I. Hall, L. Avaldi, G. Dawber, A. G. McConkey, M. A. MacDonald, and G. C. King, Chem. Phys. **187**, 125 (1994).
[4] A. S. Sandhu et al., Science **322**, 1081 (2008).
[5] J. Eland, Chem. Phys. **323**, 391 (2006).
[6] R. Dörner et al., Phys. Rep. **330**, 95 (2000).
[7] J. Ullrich, R. Moshammer, A. Dorn, R. Dörner, L. Ph. H. Schmidt, and H. Schmidt-Böcking, Rep. Prog. Phys. **66**, 1463 (2003).
[8] T. Jahnke, Th. Weber, T. Osipov, A. L. Landers, O. Jagutzki, L. Ph. H. Schmidt, C. L. Cocke, M. H. Prior, H. Schmidt-Böcking, and R. Dörner, J. Electron Spectrosc. Relat. Phenom. **141**, 229 (2004).
[9] O. Jagutzki et al., Nucl. Instrum. Methods Phys. Res., Sect. A **477**, 244 (2002).
[10] W. C. Wiley and I. H. McLaren, Rev. Sci. Instrum. **26**, 1150 (1955)
[11] O. Jagutzki et al., IEEE Trans. Nucl. Sci. **49**, 2477 (2002).
[12] J. S. Briggs and V. Schmidt, J. Phys. B **33**, R1 (2000).
[13] T. N. Rescigno, B. H. Lengsfield, and C. W. McCurdy, in "Modern Electronic Structure", edited by David Yarkony (World Scientific Publishing, Singapore, 1995), p. 501.
[14] B. D. Rehfuss, M. Jagod, L. Xu, and T. Oka, J. Mol. Spectrosc. **151**, 59 (1992).
[15] K. Zähringer, H.-D. Meyer, and L. S. Cederbaum, Phys. Rev. A **46**, 5643 (1992).
[16] N. A. Cherepkov et al., Phys. Rev. A **82**, 023420 (2010).
[17] T. Weber et al., Phys. Rev. Lett. **90**, 153003 (2003).
[18] J. L. Dehmer and D. Dill, Phys. Rev. Lett. **35**, 213 (1975); A. Landers et al., Phys. Rev. Lett. **87**, 013002 (2001).
[19] H. C. Poon and S. Y. Tong, Phys. Rev. B **30**, 6211 (1984).